

**This is an electronic reprint of the original article.
This reprint *may differ* from the original in pagination and typographic detail.**

Author(s): Kinnunen, Sami; Malm, Jari; Arstila, Kai; Lahtinen, Manu; Sajavaara, Timo

Title: Characterization of ALD grown TixAlyN and TixAlyC thin films

Year: 2017

Version:

Please cite the original version:

Kinnunen, S., Malm, J., Arstila, K., Lahtinen, M., & Sajavaara, T. (2017).
Characterization of ALD grown TixAlyN and TixAlyC thin films. Nuclear Instruments
and Methods in Physics Research Section B: Beam Interactions with Materials and
Atoms, 406(Part A), 152-155. <https://doi.org/10.1016/j.nimb.2016.12.032>

All material supplied via JYX is protected by copyright and other intellectual property rights, and duplication or sale of all or part of any of the repository collections is not permitted, except that material may be duplicated by you for your research use or educational purposes in electronic or print form. You must obtain permission for any other use. Electronic or print copies may not be offered, whether for sale or otherwise to anyone who is not an authorised user.

Characterization of ALD Grown $\text{Ti}_x\text{Al}_y\text{N}$ and $\text{Ti}_x\text{Al}_y\text{C}$ Thin Films

S.A. Kinnunen^a, J. Malm^a, K. Arstila^a, M. Lahtinen^b, T. Sajavaara^a

^a*University of Jyväskylä, Department of Physics, P. O. Box 35, FI-40014 University of Jyväskylä, Finland*

^b*University of Jyväskylä, Department of Chemistry, P.O. Box 35, FI-40014 University of Jyväskylä, Finland*

Abstract

Atomic layer deposition (ALD) was used to grow $\text{Ti}_x\text{Al}_y\text{N}$ and $\text{Ti}_x\text{Al}_y\text{C}$ thin films using trimethylaluminum (TMA), titanium tetrachloride and ammonia as precursors. Deposition temperature was varied between 325 °C and 500 °C. Films were also annealed in vacuum and N_2 -atmosphere at 600–1000 °C. Wide range of characterization methods was used including time-of-flight elastic recoil detection analysis (ToF-ERDA), X-ray diffractometry (XRD), X-ray reflectometry (XRR), Raman spectroscopy, ellipsometry, helium ion microscopy (HIM), atomic force microscopy (AFM) and 4-point probe measurement for resistivity. Deposited films were roughly 100 nm thick and contained mainly desired elements. Carbon, chlorine and hydrogen were found to be the main impurities.

Keywords: ALD, MAX-phases, ToF-ERDA

1. Introduction

Atomic layer deposition is a widely used technique to produce uniform and conformal thin films even on high-aspect-ratio structures [1]. ALD-process

4 contains sequential gas-phase precursor pulses divided by inert-gas purging.
5 Volatile precursors react on substrate and form new film layer-by-layer which
6 allows precise thickness control.

7 MAX-phases are a group of ternary carbides and nitrides that share prop-
8 erties common to both metals and ceramics. They were discovered already
9 in the 1960's [2] although more systematic research began in the 1990's and
10 currently some 60 different MAX-phases are known [3]. While many of them
11 are heat and oxidation resistant like ceramics, they often possess metal-like
12 thermal and electrical properties. MAX-phases have a common $M_{n+1}AX_n$
13 structure where $n=1, 2$ or 3 . In the formula M designates early transition
14 metal, A is an A- group element and X is carbon or nitrogen. MAX-phases
15 have layered structure where MX-layers are separated by A-layers and thick-
16 ness of MX-layer depends on n . This laminate-like structure makes most
17 MAX-phases stiff and shock resistant.

18 In this work targeted MAX-phase thin films were Ti_2AlN , Ti_4AlN_3 , Ti_2AlC
19 and Ti_3AlC_2 .

20 MAX-phase thin films have been deposited using several different meth-
21 ods like sputtering, cathodic arc deposition, chemical vapor deposition etc.
22 [3]. Deposition of MAX-phase thin films has required deposition tempera-
23 tures around $1000\text{ }^\circ\text{C}$. If deposition temperature is relatively low, post an-
24 nealing can be used to produce MAX-phases [4]. However, ALD has not
25 been utilized in making of MAX-phase thin films. Potentially, ALD could be
26 used to deposit MAX-phases in lower temperatures due to its characteristic
27 layer-by-layer deposition process.

28 **2. Experimental details**

29 All thin films were deposited using Beneq TFS-200 reactor at 1–2 mbar
30 pressure on $\langle 100 \rangle$ silicon substrate. TiCl_4 , TMA and NH_3 were used as
31 precursors to deposit $\text{Ti}_x\text{Al}_y\text{N}$ films by mixing TiN and AlN cycles. In ad-
32 dition, $\text{Ti}_x\text{Al}_y\text{C}$ films were deposited using solely TiCl_4 and TMA. Nitrogen
33 was used as a carrier and purge gas in both cases. TiN/AlN cycle consisted
34 of 150 ms TiCl_4 /TMA pulse, 750 ms purge, 300 ms NH_3 pulse and 2000 ms
35 purge. Nitride films were deposited at 325, 400 and 450 °C. When deposit-
36 ing nitride films, ratio of TiN and AlN cycles were varied in order to achieve
37 different atomic composition. Carbide cycle consisted of 300 ms TMA pulse,
38 2000 ms purge, 150 ms TiCl_4 pulse and 1000 ms purge, and deposition was
39 done at 500 °C. In order to compensate relatively low deposition tempera-
40 ture for MAX-phases, as deposited films were also annealed in vacuum and
41 nitrogen atmosphere at 600–1000 °C for 10 minutes.

42 Elemental composition was determined using 1.7 MV Pelletron acceler-
43 ator by ToF-ERDA with 13.615 MeV $^{63}\text{Cu}^{7+}$ incident ions [5]. Heavy ions
44 were accelerated in order to produce recoiled atoms from the sample. In ToF-
45 ERDA, time-of-flight (velocity) and energy of recoiled atoms are measured
46 and different masses can be separated. When stopping forces, scattering
47 cross-sections and measurement geometry are known, data can be used to
48 produce elemental depth profiles. Even the lightest elements including hy-
49 drogen can be detected. [6]

50 Surface morphology and cross-sections of the films were investigated with
51 Zeiss Orion Nanofab helium ion microscope. Surface roughness was measured
52 with Digital Instruments, Dimension 3100 (NanoScope IV and V) Bruker

53 (Veeco) atomic force microscope.

54 Crystallinity of the films was investigated using XRD (PANalytical X’Pert
55 Pro) with copper $K_{\alpha 1}$ X-rays. Film thicknesses and densities were measured
56 with the same equipment using XRR-configuration.

57 Raman measurements were made with home build Raman setup using
58 532 nm excitation with back scattering geometry.

59 **3. Results**

60 Growth per cycle (GPC) of binary TiN and AlN at 450 °C were 0.36 Å/cycle
61 and 1.9 Å/cycle, respectively. Mixing of TiN and AlN cycles did not have
62 an effect on growth rates of individual cycles. TiN and AlN GPCs at 325 °C
63 were 0.30 Å/cycle and 0.16 Å/cycle. Similar growth rates for AlN have been
64 reported [7], although GPC reported in this work at 450 °C is relatively high.
65 High growth rate can be due to decomposing TMA, which starts at 332 °C
66 [8]. This may lead to more continuous CVD-growth instead of self-limiting
67 ALD-growth. Growth rate of TiN was somewhat higher than reported else-
68 where, for example Ahn *et al.* reported 0.17 Å/cycle [9] and Satta *et al.*
69 0.24–0.28 Å/cycle at 400 °C [10]. For Ti_xAl_yN films deposited at 325 °C
70 the average TiN/AlN GPC was 0.45 Å/cycle and the average GPC was in-
71 dependent of TiN:AlN cycle ratio. The average growth per subcycle was
72 higher than for either binary compound. This growth enhancing can be due
73 to TMA, which can act as an extra reducing agent for TiN [11].

74 Densities of the binary films are lower than bulk densities of TiN and
75 AlN (5.21 g/cm³ and 3.255 g/cm³ [12], respectively), as seen in Table 1. In-
76 creasing deposition temperature slightly increases film density, and densities

Table 1: Density, surface roughness and elemental composition of as deposited films. TiN:AlN cycle ratio is mentioned for Ti_xAl_yN films. Interface and surface region are excluded from composition analysis due to surface oxygen. Relative uncertainty for main components is 2 %, for impurities excluding hydrogen 5 % and for hydrogen 10 %.

Film	T [°C]	Density [g/cm ³]	RMS roughness [nm]	Ti	Al	N	O	C	Cl	H	Other
TiN	325	4.23	-	45	-	53	0.3	0.1	1.3	0.4	Na 0.2
AlN	325	2.15	1.2	-	36	39	2.9	1.5	0.5	20	-
$TiAl_xN_y$ 1:2	325	3.40	0.6	22	16	43	<0.1	3.1	5.9	10	-
$TiAl_xN_y$ 1:1	325	3.79	0.5	30	10	42	0.2	5.3	5.7	6.8	-
$TiAl_xN_y$ 4:3	325	3.74	0.3	32	9.0	41	<0.1	5.7	5.6	6.3	-
$TiAl_xN_y$ 1:1	400	-	-	22	23	47	0.1	3.0	1.4	3.5	-
TiN	450	4.70	0.8	45	-	53	0.6	0.1	0.1	<0.1	Na 0.2
AlN	450	-	2.1	-	43	43	0.2	4.2	-	9.7	-
$TiAl_xN_y$ 1:2	450	3.18	1.9	7.3	36	43	0.1	6.2	1.4	6.1	-
$TiAl_xN_y$ 1:1	450	4.07	-	24	20	45	0.1	7.9	0.8	2.7	-
$TiAl_xN_y$ 2:1	450	4.26	0.4	30	14	47	0.1	6.0	0.8	1.5	-
$TiAl_xN_y$ 4:1	450	4.57	0.4	36	8.0	46	0.1	7.7	0.8	1.8	-
$TiAl_xC_y$	500	3.18	1.1	26	6.2	-	0.1	62	2.3	3.7	-

77 of Ti_xAl_yN -films fall between binary compounds.

78 Surface root mean square roughness of the films was relatively low and
79 varied from 0.3 to 2.1 nm (Table 1). Acquired AFM topographs did not show
80 signs of crystallization.

81 Elemental compositions of as deposited films are presented in Table 1.
82 Example of acquired time-of-flight and energy histogram is presented in Fig-
83 ure 1 a). As deposited films had uniform elemental composition with thin
84 oxide layer at the surface. A representative example is presented in Figure 1
85 b).

86 Elemental depth profiles acquired by ToF-ERDA measurements show that
87 films grow homogeneously and contain mainly desired elements. Ratio be-
88 tween titanium and aluminum can be controlled by selecting desired amount
89 of TiN and AlN subcycles. Ti:Al ratio in the film is linearly dependent on

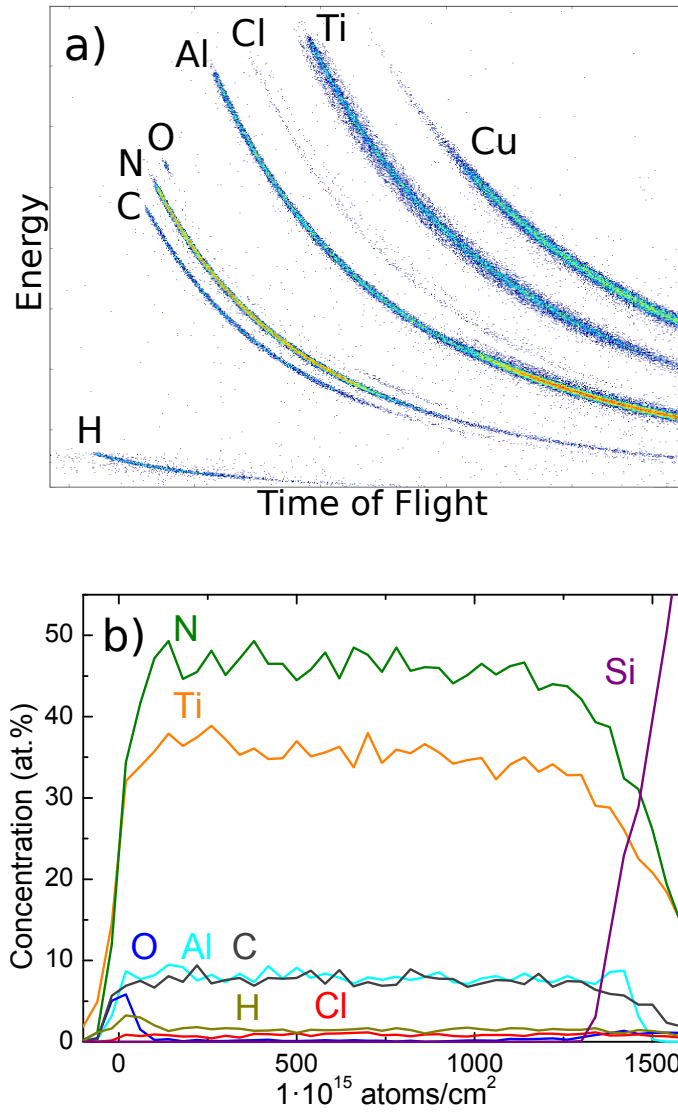


Figure 1: a) Coincidence time of flight and energy histogram. For Ti_xAl_yN film deposited at 450 °C with TiN:AlN cycle ratio of 4:1, different elements can be separated and identified. b) Corresponding elemental depth profile.

90 TiN:AlN subcycle ratio but varies with deposition temperature as seen in Fig-
91 ure 2. The nitrogen content was not affected by cycle ratios or deposition
temperature, and was between 41–47 at.%. Main impurities in the films

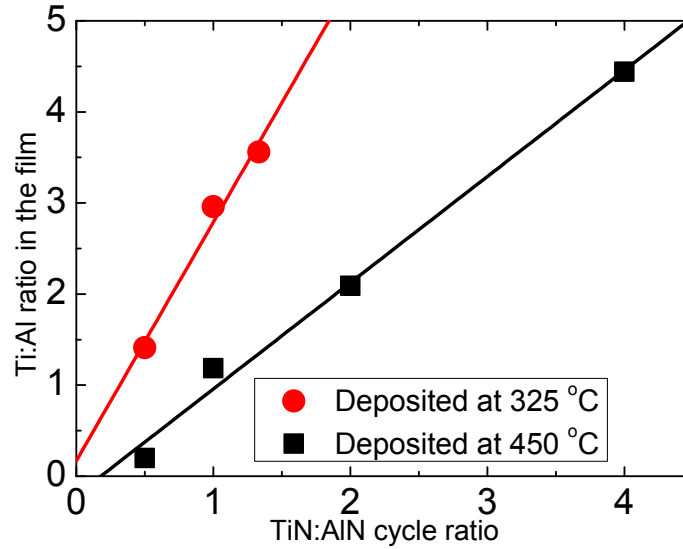


Figure 2: Ti:Al ratio in the Ti_xAl_yN films as a function of TiN:AlN cycle ratio at two different deposition temperature.

92
93 were carbon, hydrogen and chlorine which originate from precursors. Small
94 amount of oxygen was detected at the film surface and interface. Increase
95 in deposition temperature decreases amount of hydrogen and chlorine due to
96 more complete surface reactions (Figure 3). However, carbon concentration
97 increases at 450 °C. TMA starts to decompose at 332 °C [8], which is the
98 probable reason for the increase of carbon at higher temperatures. Anneal-
99 ing of films in vacuum had little effect on film composition or crystallinity.
100 Some chlorine and hydrogen was removed but main components of the film
101 remained unchanged.

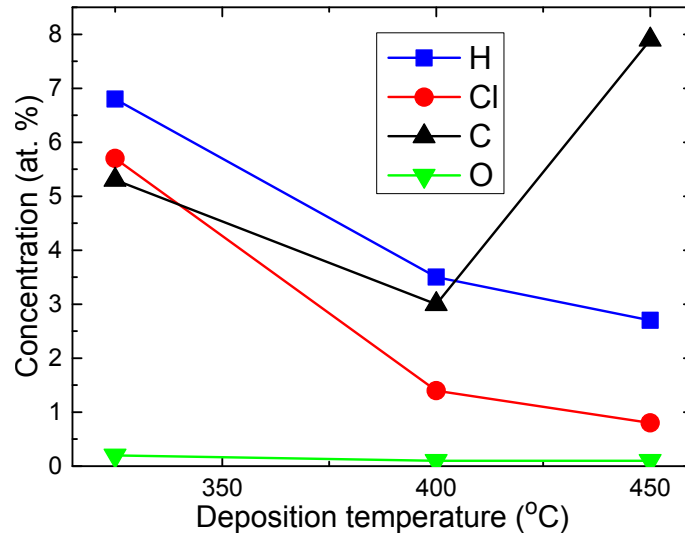


Figure 3: Impurity concentrations of Ti_xAl_yN films deposited at different temperatures.

102 Films annealed at N_2 -atmosphere were oxidized due to unknown oxygen
 103 source. Relative amounts of main components remained unchanged after
 104 annealing, while impurity concentrations excluding oxygen decreased slightly.

105 ToF-ERD analysis showed that films deposited at 450 °C were more oxida-
 106 tion resistant than films deposited at 325 °C. During annealing aluminum
 107 accumulates at film surface where it forms aluminum oxide which can be
 108 seen in Figure 4 a). Protective aluminum oxide layer is formed independent
 109 of deposition temperature. However, oxygen incorporates films deposited at
 110 325 °C thoroughly as seen in Figure 4 b), while oxidation stopped after few
 111 tens of nanometers in films deposited at 450 °C.

112 According to XRD-measurements, as deposited films as well as annealed
 113 films were mostly amorphous containing only small crystals. No detectable
 114 MAX-phases were found. Cubic TiN and wurtzite-like AlN crystals with

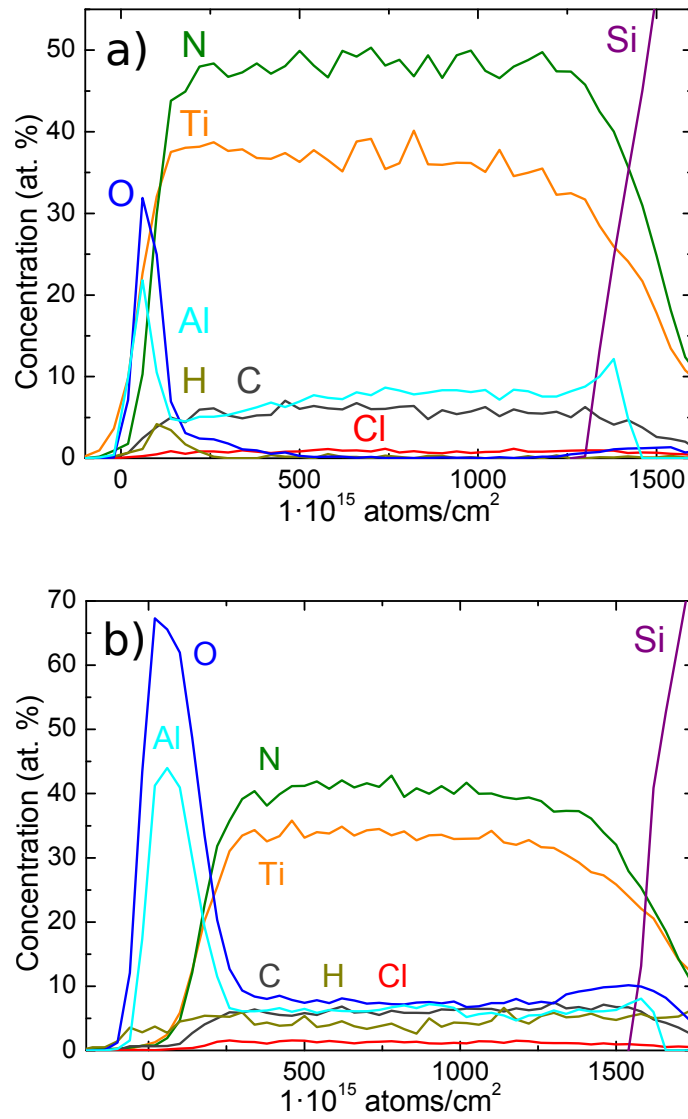


Figure 4: a) Depth profile of a Ti_xAl_yN film (4:1) deposited at 450 °C after 10 minute annealing in N₂-atmosphere at 1000 °C. b) Depth profile of Ti_xAl_yN film (4:3) deposited at 325 °C after 10 minute annealing in N₂-atmosphere at 1000 °C.

115 average size around 10 nm were detected. Annealing increased slightly crys-

116 tallinity of the films but did not cause formation of MAX-phases. Likewise,
117 Raman spectroscopy could not find traces of MAX-phases. However, ac-
118 cording to Raman measurements impurity carbon seems to form C–C double
119 bonds during annealing. Home made 4-point probe was used to determine
120 resistivity of the films. Films deposited at 325 °C had resistivity at $10^{-5} \Omega\text{m}$
121 region while films deposited at 450 °C had resistivity roughly one order of
122 magnitude lower. Resistivity decreased with increasing titanium concentra-
tion.

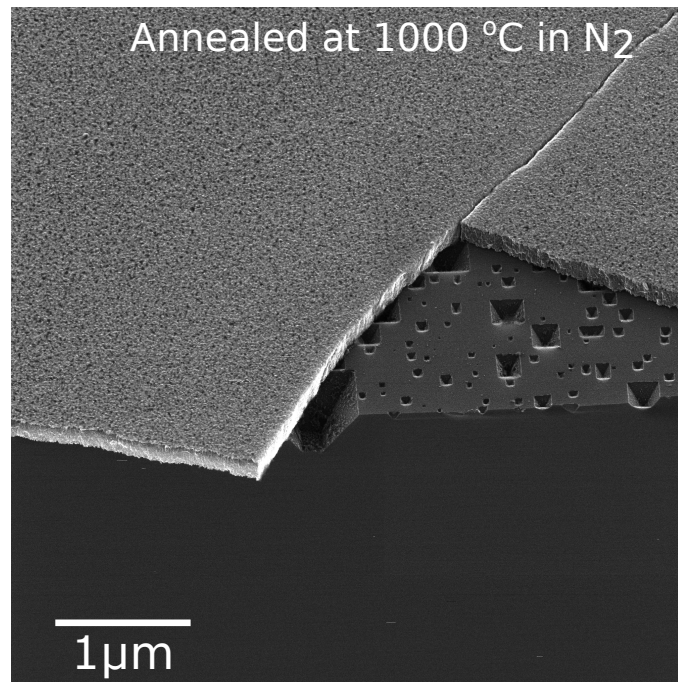


Figure 5: HIM micrograph of $\text{Ti}_x\text{Al}_y\text{N}$ film deposited at 325 °C after annealing in N_2 -atmosphere at 1000 °C. Sample is tilted at 45°.

123

124 HIM micrographs revealed unexpected anisotropic etching of silicon wafer
125 underneath the film after annealing in N_2 -atmosphere. Micrograph of $\text{Ti}_x\text{Al}_y\text{N}$

126 film after annealing is seen in Figure 5. Etching seems to take place only in
 127 the films deposited at 325 °C and not in the films deposited at 450 °C. Strong
 128 bases which typically contain hydroxyl group are used to anisotropically etch
 129 silicon [13]. It could be possible, that oxygen which penetrated films de-
 130 posited at 325 °C during annealing (Figure 4 b)), forms OH⁻ -groups with
 131 impurity hydrogen. These hydroxyl groups could possibly cause anisotropic
 132 etching.

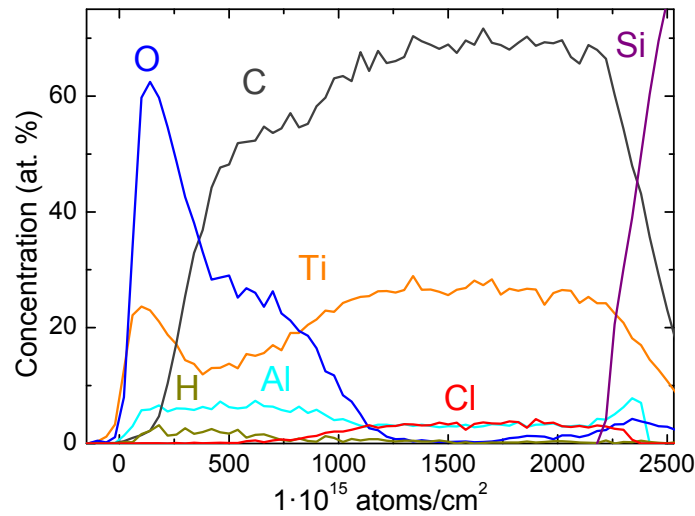


Figure 6: Elemental depth profile of Ti_xAl_yC film after annealing in N_2 -atmosphere at 1000 °C.

133 Ti_xAl_yC films were successfully deposited and elemental composition was
 134 uniform. Films were carbon rich and contained only little aluminum (see
 135 Table 1). Growth rate of Ti_xAl_yC was 1.5 Å/cycle. Films contained TiC
 136 crystals with average size less than 10 nm and no MAX-phases could be
 137 identified. Annealing of the film in N_2 -atmosphere also lead to oxidation of
 138 the film similar to nitride films. Interestingly, titanium accumulates in the

139 surface as an oxide, while aluminum seems to form a second layer on the
140 surface with titanium oxide layer, as seen in Figure 6. Rutile (TiO_2) crystals
141 were detected by XRD in annealed carbide films.

142 **4. Conclusions**

143 Titanium and aluminum concentration in $\text{Ti}_x\text{Al}_y\text{N}$ films can be controlled
144 by varying TiN and AlN pulse ratios. Nitrogen content in the films remained
145 approximately constant and it was too high considering MAX-phases. Impu-
146 rity concentrations decreased with increasing deposition temperature exclud-
147 ing carbon. Films deposited at 450 °C were more resistant to oxidation com-
148 pared to films deposited at lower temperature. During annealing aluminum
149 seems to accumulate in the film surface yielding a protective aluminum ox-
150 ide layer. Films were mostly amorphous containing only small TiN and AlN
151 crystals while no MAX-phases were detected. Unexpected anisotropic etch-
152 ing of the $\langle 100 \rangle$ silicon wafer underneath $\text{Ti}_x\text{Al}_y\text{N}$ film deposited at 325 °C
153 was discovered, after films were annealed in N_2 at 1000 °C.

154 In addition carbon rich $\text{Ti}_x\text{Al}_y\text{C}$ films were deposited and annealed. Alu-
155 minum content in carbide films was too low for MAX-phases. Films contained
156 small TiC crystals but no trace of MAX-phases.

157 **Acknowledgments**

158 This work was supported by Academy of Finland Center of Excellence in
159 Nuclear and Accelerator Based Physics (Ref. No. 251353).

160 **References**

- 161 [1] V. Miikkulainen, M. Leskelä, M. Ritala, and R. Puurunen. *Crystallinity*
162 *of inorganic films grown by atomic layer deposition: Overview and gen-*
163 *eral trends*. Journal of Applied Physics, 113, 021301 (2013)
- 164 [2] H. Nowotny. *Strukturchemie einiger Verbindungen der Übergangsmetalle*
165 *mit den elementen C, Si, Ge, Sn*. Progress in Solid State Chemistry, 5,
166 (1971)
- 167 [3] P. Eklund, M. Beckers, U. Jansson, H. Högberg, and L. Hultman. *The*
168 *$M_{n+1}AX_n$ phases: Materials science and thin film processing*. Thin Solid
169 Films, 518(8):1851–1878, (2010).
- 170 [4] R. Grieseler, T. Kups, M. Wilke, M. Hopfeld and P. Schaaf. *Formation*
171 *of Ti_2AlN nanolaminate films by multilayer-deposition and subsequent*
172 *rapid thermal annealing*. Materials Letters, 82, 74–77 (2012)
- 173 [5] M. Laitinen, M. Rossi, J. Julin and T. Sajavaara. *Time-of-flight – En-*
174 *ergy spectrometer for elemental depth profiling – Jyväskylä design* Nucl.
175 Instrum. Meth. B 337, 55–61 (2014)
- 176 [6] M. Putkonen, T. Sajavaara, L. Niinistö and J. Keinonen. *Analysis of*
177 *ALD-processed thin films by ion-beam techniques*. Analytical and Bioan-
178 alytical Chemistry, 382 (2005)
- 179 [7] C. Ozgit, I. Donmez, M. Alevli, and N. Biyikli. *Self-limiting low-*
180 *temperature growth of crystalline AlN thin films by plasma-enhanced*
181 *atomic layer deposition*. Thin Solid Films, 520(7):2750–2755 (2012)

- 182 [8] S. Yamashita, K. Watanuki, H. Ishii, Y. Shiba, M. Kitano, Y. Shirai, S.
183 Sugawa, and T. Ohmi. *Dependence of the Decomposition of Trimethylal-*
184 *uminium on Oxygen Concentration*. Journal of Electrochemical Society,
185 158(2):93–96, (2011)
- 186 [9] C. Ahn, S. Cho, H. Lee, K. Park, and S. Jeong. *Characteristics of TiN*
187 *thin films grown by ALD using $TiCl_4$ and NH_3* . Metals and Materials
188 International, 7(6):621–625 (2001)
- 189 [10] A. Satta, J. Schuhmacher, C. Whelan, W. Vandervorst, S. Brongersma,
190 G. Beyer, K. Maex, A. Vantomme, M. Viitanen, H. Brongersma, and W.
191 Besling. *Growth mechanism and continuity of atomic layer deposited TiN*
192 *films on thermal SiO_2* . Journal of Applied Physics, 7641–7646 (2002)
- 193 [11] V. Juppo, P. Alén, M. Ritala, and M. Leskelä. *Trimethylaluminium as a*
194 *Reducing Agent in the Atomic Layer Deposition of $Ti(Al)N$ Thin Films*.
195 Chem. Vap. Deposition, 7, 211 (2001)
- 196 [12] David R. Lide. *CRC Handbook of Chemistry and Physics, 85th edition*.
197 CRC Press, Boca Raton, 2005
- 198 [13] H. Seidel, L. Csepregi, A. Heuberger and H. Baumgärtel. *Anisotropic*
199 *Etching of Crystalline Silicon in Alkaline Solutions*. J. Electrochem. Soc.
200 137:3612 (1990)